Synthesis of a Benzoxazine with Precisely Two Phenolic OH Linkages and the Properties of Its High-Performance Copolymers

Ching Hsuan Lin,[1] Yu Ren Feng,[1] Kang Hong Dai,[1] Hou Chien Chang,[1] Tzong Yuan Juang[2]

[1]Department of Chemical Engineering, National Chung Hsing University, Taichung, Taiwan
[2]Department of Applied Chemistry, National Chiayi University, Chiayi, Taiwan
Correspondence to: C. H. Lin (E-mail: linch@nchu.edu.tw) or H. C. Chang (E-mail: hchang@dragon.nchu.edu.tw)

Received 28 December 2012; accepted 23 February 2013; published online 29 March 2013
DOI: 10.1002/pola.26661

ABSTRACT: A phenolic OH-containing benzoxazine (**F-ap**), which cannot be directly synthesized from the condensation of bisphenol F, aminophenol, and formaldehyde by traditional procedures, has been successfully prepared in our alternative synthetic approach. **F-ap** was prepared by three steps including (a) condensation of 4-aminophenol and 5,5′-methylenebis(2-hydroxybenzaldehyde) **(1)**, (b) reduction of the resulting imine linkage by sodium borohydride, and (c) ring closure condensation by formaldehyde. The key starting material, **(1)**, was prepared from 2-hydroxybenzaldehyde and s-trioxane in the presence of sulfuric acid. **F-ap** is structurally similar to bis(3,4-dihydro-2H-3-phenyl-1,3-benzoxazinyl)methane (**F-a,** a commercial benzoxazine based on bisphenol F/aniline/formaldehyde) except for two phenolic OHs. The phenolic OHs can provide reaction sites with epoxy and 1,1′-(methylenedi-p-phenylene)bismaleimide (BMI). The structure–property relationships between the thermosets of **F-ap**/epoxy, **F-a**/epoxy, **F-ap**/BMI, and **F-a**/BMI were discussed. Experimental data showed that thermosets based on **F-ap**/epoxy and **F-ap**/BMI provided much better thermal properties than those based on **F-a**/epoxy and **F-a**/BMI. © 2013 Wiley Periodicals, Inc. J. Polym. Sci., Part A: Polym. Chem. **2013**, *51*, 2686–2694

KEYWORDS: high performance polymers; synthesis; thermosets

INTRODUCTION Benzoxazines are resins that can be polymerized to thermosets by means of thermally activated ring-opening reactions.[1] Thermosets with low water absorption, superior electrical properties,[2] and low surface energy[3] can be obtained after curing. Bifunctional benzoxazine monomers are generally prepared from bisphenols, mono primary amine, and formaldehyde at a molar ratio of 1:2:4. The wide variety of aromatic bisphenols and monoamines allow for considerable flexibility in the molecule-design of benzoxazines. Some special functional groups, such as acetylene,[4,5] furan,[6] allyl,[7] propargyl,[8] vinyl,[9] amide,[10] phenol,[11] maleimide,[12] carboxylic acid,[13] methacrylol,[14] thymine,[15] and amine[16] have been incorporated into benzoxazines to provide the desired physical properties. Recently, Endo et al. reported that polymer bearing 1,3-benzoxazine moiety in the side chain was synthesized based on a stepwise strategy.[17] However, precise synthesis of a bifunctional benzoxazine monomer with phenolic OHs in its structure is a challenge in benzoxazine synthesis.[18] For example, it is difficult to prepare a phenolic OH-containing benzoxazine from bisphenol F, aminophenol, and formaldehyde because the Mannich-type polycondensation of aminophenol and formaldehyde lead to polybenzoxazine precursors with M_w ranging from 1300 to 4500 g/mol.[19]

It has been reported that incorporation of the maleimide group into benzoxazine can improve the thermal properties of the resulting thermosets.[20–22] Takeichi et al. reported a thermal reaction between the phenolic OH (resulting from the ring-opened polybenzoxazine) and maleimide, as supported by the model reaction of phenol and *N*-phenylmaleimide.[23] Based on their finding, they successfully incorporated bismaleimide into a polybenzoxazine matrix to achieve high-performance alloys. We suspect that a benzoxazine with phenolic OHs can provide extra reaction sites with maleimide linkages of 1,1′-(methylenedi-*p*-phenylene)bismaleimide (BMI). In addition, it is known that phenolic OH can also provide a reaction site with epoxy. Therefore, high-performance benzoxazine/BMI and benzoxazine/epoxy thermosets can be expected to result from a phenolic OH-containing benzoxazine.

In this study, we provide a strategy for preparing a phenolic OH-containing benzoxazine **(F-ap)** (In this facile nomenclature of benzoxazine, "F" stands for bisphenol F, and "ap" stands for aminophenol). **F-ap** is structurally similar to bis(3,4-dihydro-2H-3-phenyl-1,3-benzoxazinyl)methane (**F-a,** a commercial benzoxazine based on bisphenol F/aniline/formaldehyde) except for two phenolic OHs. We prepare thermosets based on **F-ap**/epoxy, **F-a**/epoxy, **F-ap**/BMI, and **F-a**/BMI. This study

Additional Supporting Information may be found in the online version of this article.

provides a detailed synthetic strategy and the structure–property relationships of the resulting thermosets.

EXPERIMENTAL

Materials

s-Trioxane (from Acros), 2-hydroxybenzaldehyde (from Showa), sulfuric acid (from Scharlau), acetic acid (from Scharlau), 4-aminophenol (from Aldrich), paraformaldehyde (from TCI), 1,1'-(methylenedi-*p*-phenylene)bismaleimide (BMI, from Acros), and sodium borohydride ($NaBH_4$, from Acros) were used as received. Diglycidyl ether of bisphenol A (DGEBA) with an epoxy equivalent weight (EEW) of 188 g/eq was kindly supplied by Chang Chun Plastics, Taiwan. Solvents were purchased from TEDIA and used without further purification.

Characterization

Differential scanning calorimetry (DSC) scans were obtained using a Perkin-Elmer DSC 7 in a nitrogen atmosphere at a heating rate of 20°C/min. Thermal gravimetric analysis (TGA) was performed with a Perkin-Elmer Pyris1 at a heating rate of 20°C/min in an atmosphere of nitrogen or air. Dynamic mechanical analysis (DMA) was performed with a Perkin-Elmer Pyris Diamond DMA with a sample size of 5.0 × 1.0 × 0.2 cm^3. The storage modulus *E'* and tan δ were determined as the sample was subjected to a temperature scan mode at a programmed heating rate of 5°C/min at a frequency of 1 Hz. The test was performed by a bending mode with an amplitude of 5 μm. Thermal mechanical analysis (TMA) was performed by a SII TMA/SS6100 at a heating rate of 5 °C/min. NMR measurements were performed using a Varian Inova 600 NMR in DMSO-d_6, and the chemical shift was calibrated by setting the chemical shift of DMSO-d_6 at 2.49 ppm. IR Spectra were obtained from at least 32 scans in the standard wavenumber range of 400–4000 cm^{-1} using a Perkin-Elmer RX1 infrared spectrophotometer.

Synthesis of (1)

s-Trioxane 10.0 g (0.111 mol), 2-hydroxybenzaldehyde 89.46 g (0.732 mol), acetic acid 100 g, and sulfuric acid 3.09 g were introduced into a 250-mL glass flask equipped with a nitrogen inlet and a magnetic stirrer. The mixture was reacted at 85°C for 22 h. After the reaction solution was cooled to room temperature, the precipitate was filtered, dissolved in methanol, and poured into water. The precipitate was filtrated and then dried in a vacuum oven at 105°C. Off-white powder (44 % yield) was obtained.

^{1}H NMR (DMSO-d_6), $\delta = 3.84$(s, 2H, H^1), 6.93(d, 2H,H^7), 7.37(d, 2H, H^8), 7.46(s, 2H, H^3), 10.22(s, 2H, H—C═O), 10.57(s, 2H,OH), ^{13}C NMR (DMSO-d_6), $\delta = 38.6$ (C^1), 117.5(C^7), 122.1 (C^6), 128.3 (C^3), 132.3 (C^2), 136.9 (C^8), 159.2(C^4), 191.3 (C^5). FTIR (KBr):1655 cm^{-1} (C═O stretch), 3425 cm^{-1} (OH stretch)

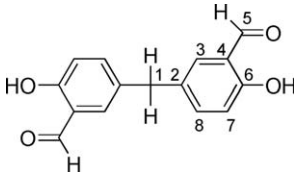

Synthesis of (2)

Five grams of (**1**) (19.5 mmol), 4-aminophenol 4.26 g (39 mol), and DMAc 50 mL were introduced into a 250-mL glass flask equipped with a hydrogen balloon and a magnetic stirrer. The mixture was reacted at 25°C for 12 h. $NaBH_4$ 0.775 g (20.48 mmol) was added every 1 h. After $NaBH_4$ was added three times (total 62.4 mmol), the reaction mixture was further stirred at room temperature for 12 h. The mixture was then poured into water. The precipitate was filtered and dried in a vacuum oven at 105°C. Yellow powder (85% yield) was obtained.

^{1}H NMR (DMSO-d_6), $\delta = 3.61$(s, 2H, H^1), 4.04(d, 4H, H^5), 5.18(t, 2H, NH), 6.45(br, 4H, H^7), 6.52(br, 4H, H^8), 6.67(br, 2H, H^{11}), 6.77(br, 2H, H^{12}), 7.03(s, 2H, H^3), 8.39(s, 2H, OH), 9.27(s, 2H, OH). ^{13}C NMR (DMSO-d_6), $\delta = 39.5$ (C^1), 43.2 (C^5), 114.8 (C^7), 114.8 (C^{11}), 115.4 (C^8), 125.8 (C^4), 127.4 (C^{12}), 128.8 (C^3), 131.9 (C^2), 141.7 (C^6), 148.4 (C^{10}), 153.2 (C^9). FTIR (KBr): 1244 cm^{-1} (C—N stretch), 3290 cm^{-1} (NH stretch), 3400 cm^{-1} (OH stretch).

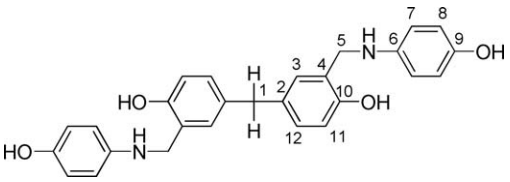

Synthesis of F-ap. (2)

Five grams (11.3 mmol), paraformaldehyde 1.09 g (36.16 mmol), and toluene 30 mL were introduced into a 100-mL round-bottom glass flask equipped with a condenser and a magnetic stirrer. The mixture was stirred at 50°C for 6 h. The precipitate was filtered, washed with *n*-hexane, and dried in a vacuum oven at 105°C. Light yellow powder (93% yield) with a melting point of 143°C (DSC) and an exothermic peak temperature of 213°C was obtained.

^{1}H NMR (DMSO-d_6), $\delta = 3.68$(s, 2H, H^1), 4.52(s, 4H, H^5), 5.24(s, 4H, H^{10}), 6.61(br, 2H, H^{12}), 6.63(br, 2H, H^7), 6.86(s, 2H, H^3), 6.91(br, 4H, H^{13}), 6.92(br, 2H, H^8), 8.96(s, 2H, OH). ^{13}C NMR (DMSO-d_6), $\delta = 39.9$ (C^1), 49.9(C^5), 79.9(C^{10}), 115.5(C^7), 116.0(C^{12}), 119.7 (C^8), 121.1(C^4), 126.9 (C^3), 127.8 (C^{13}) 133.4(C^2), 140.4 (C^6), 152.2 (C^9), 151.9 (C^{11}), FTIR (KBr):954 cm^{-1}, 1040 cm^{-1}, 1240 cm^{-1}, 1370 cm^{-1}.

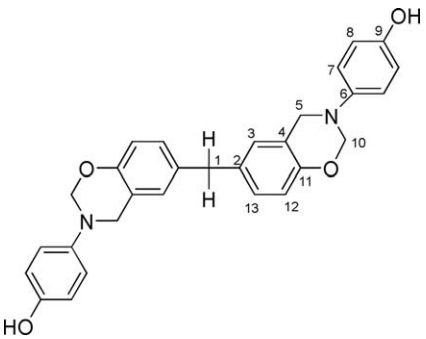

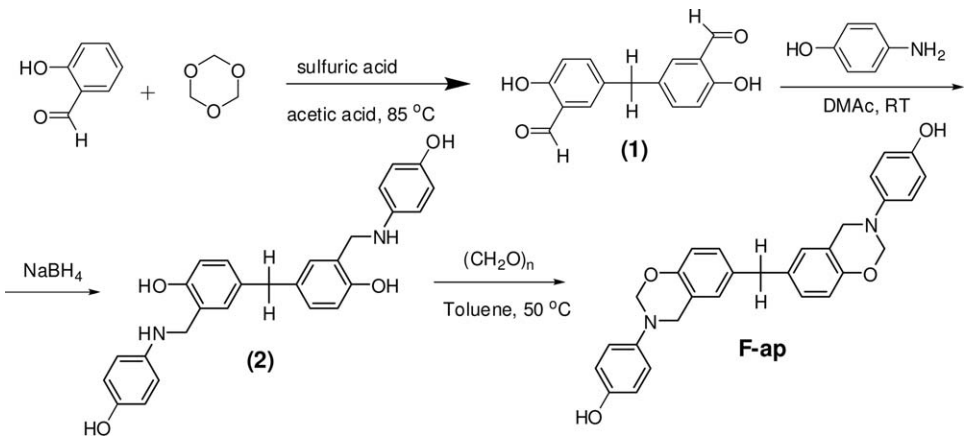

SCHEME 1 Synthesis of **F-ap**.

Preparation of Thermosets

A powder mixture of **F-ap**/BMI with equal equivalency was stirred at 160°C in an aluminum mold and cured for 2 h at 180, 200, 220, and 240°C in an air-circulating oven (Note that four phenolic OHs are generated after the ring-opening of each **F-ap** molecule, so the equivalency of **F-ap** is 116 g/eq). Thereafter, the **F-ap**/BMI thermoset was allowed to cool slowly to room temperature to prevent cracking. Thermosets of **F-a**/BMI, **F-ap**/DGEBA, and **F-a**/DGEBA were prepared using the same procedure as that used for the **F-ap**/BMI thermoset. (Note that two phenolic OHs are generated after the ring-opening of each **F-a** molecule, so the equivalency of **F-a** is 217 g/eq).

RESULTS AND DISCUSSION

Synthesis of F-ap

A phenolic OH-containing benzoxazine (**F-ap**), which cannot be directly prepared from bisphenol F/aminophenol/formaldehyde by traditional procedures, has been successfully prepared by a three-step procedure (Scheme 1).[24,25] The key starting material, 5,5'-methylenebis(2-hydroxybenzaldehyde) **(1)**, was prepared from 2-hydroxybenzodehyde and s-trioxane in the presence of sulfuric acid.[26] Supporting Information Figure S1 shows the ^{1}H NMR spectrum of **(1)**. Methylene at 3.84 ppm, aldehyde (H^5) at 10.2 ppm, and phenolic OH at 10.6 ppm were clearly observed. An enlarged NMR spectrum shows that H^7 is a doublet, H^8 is a doublet-

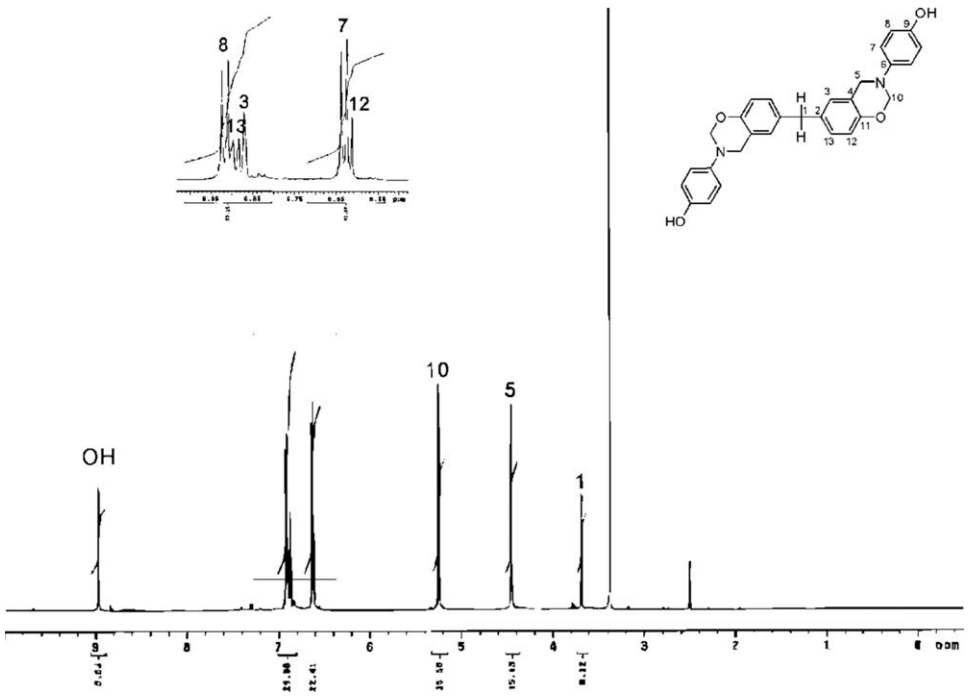

FIGURE 1 ^{1}H NMR spectrum of **F-ap** in DMSO-d_6.

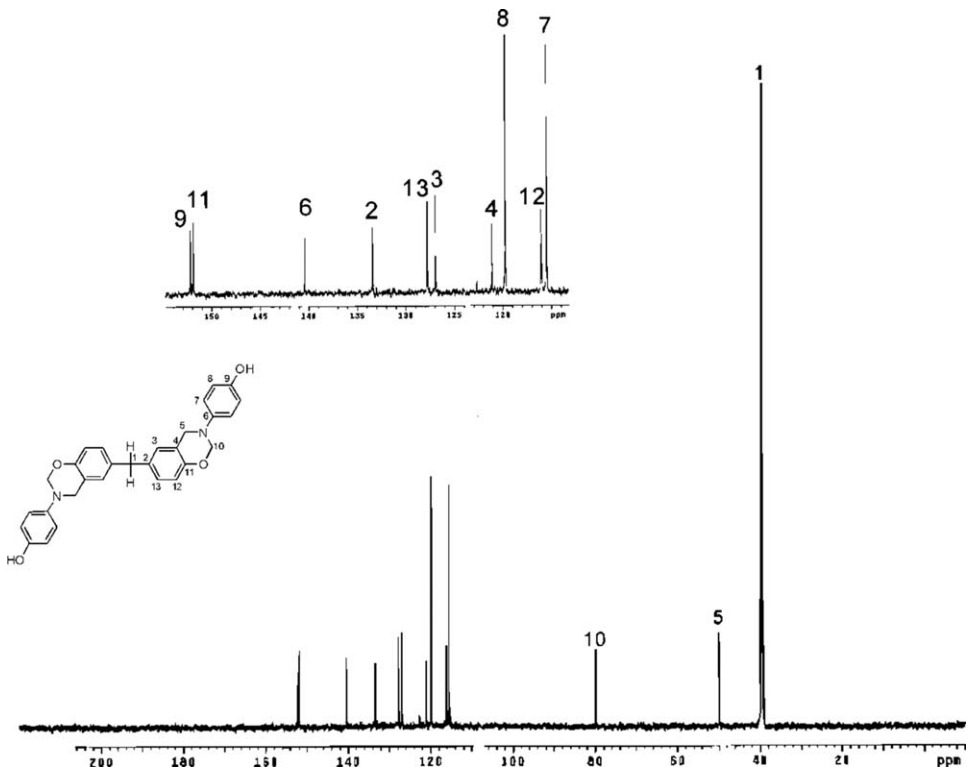

FIGURE 2 ^{13}C NMR spectrum of **F-ap** in DMSO-d_6.

doublet, and H^3 is a doublet, further confirming the structure of **(1)**. In the ^{13}C NMR spectrum (Supporting Information Figure S2), the methylene (C^1) at 38.6 ppm, and aldehyde at 191.3 ppm were clearly evident.

In the second step, **(1)** reacted with aminophenol, yielding a bis(*o*-hydroxyphenylimine) linkage. Sodium borohydride was then employed to reduce the imine linkage, yielding **(2)**. Supporting Information Figure S3 shows the ^1H NMR spectrum of **(2)**. Two signals of phenolic OH at 8.4 and 9.3 ppm were observed. Moreover, two new peaks appeared at 5.2 and 4.0 ppm, standing for CH_2—N**H** and C**H$_2$**—NH, respectively. In the ^{13}C NMR spectrum (Supporting Information Figure S4), the methylene (C^5) at 43.2 ppm, and two Ar-OH carbons (C^9 and C^{10}) at 148.4 and 153.2 ppm were clearly evident.

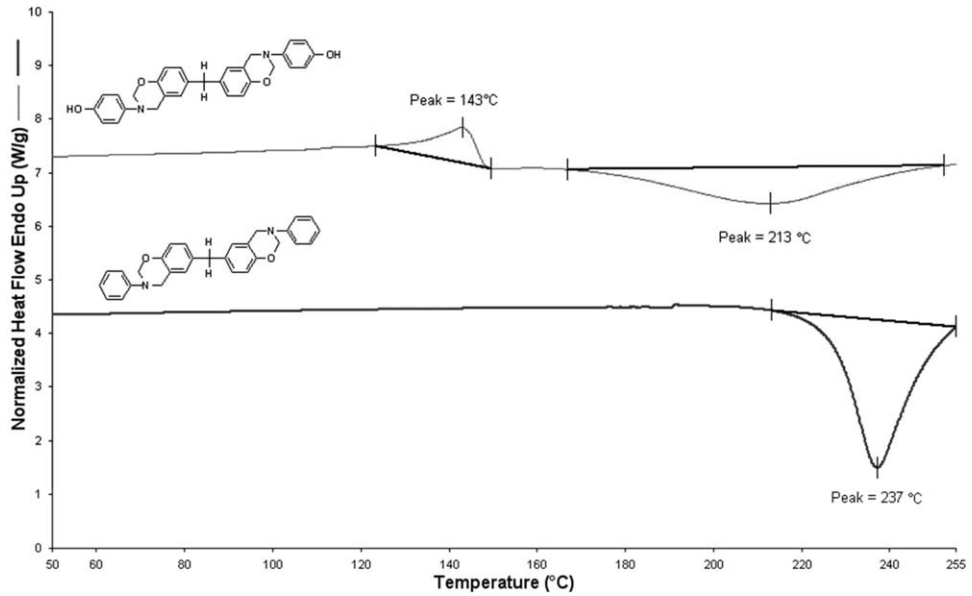

FIGURE 3 DSC thermograms of **F-ap** and **F-a**.

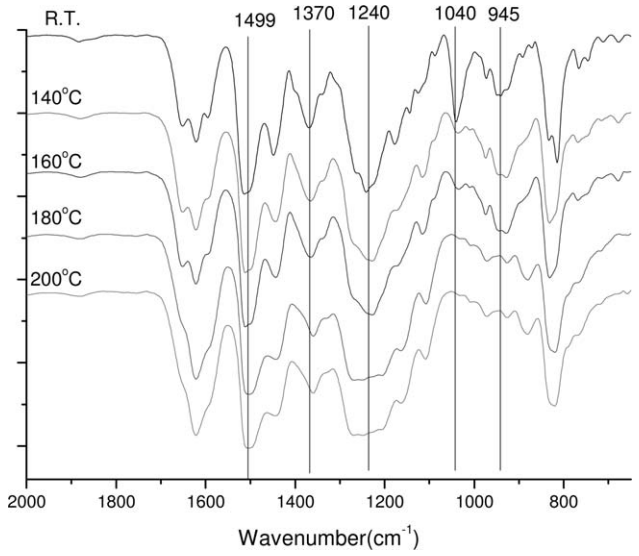

FIGURE 4 IR spectra of **F-ap** after accumulative curing at each temperature for 20 min.

In the last step, paraformaldehyde was added to the toluene solution of **(2)** to induce ring closure condensation. Supporting Information Figure S5 shows the IR spectra of **(2)** and **F-ap**. The sharp NH absorption at 3300 cm^{-1} disappeared, and new absorptions appeared at 945 cm^{-1} (the out-of-plane mode of the benzoxazine ring to which the oxazine ring is attached, 1040 (Ar—O—C symmetric stretch), 1240 (Ar—O—C asymmetric stretch) and 1370 cm^{-1} (oxazine). Figure 1 shows the ^1H NMR spectrum of **F-ap**. The characteristic peaks of benzoxazine, O—C**H**$_2$—N (H^{10}) and ph—C**H**$_2$—N (H^5), were observed at 5.2 and 4.5 ppm, respectively. No signal was observed at around 4.0 ppm corresponding to the N—C**H**$_2$—ph resulting from the ring opened benzoxazine, revealing the purity of the synthesized benzoxazine. The signal of phenolic OH was observed at 9.0 ppm. All signals of Ar-H (H^3, H^7, H^8, H^{12}, and H^{13}) were clearly assigned. Figure 2 shows the ^{13}C NMR spectrum of **F-ap**. The characteristic peaks of benzoxazine at 49.9 (ph—C**H**$_2$—N, C^5) and 79.9 (O—C**H**$_2$—N, C^{10}) ppm confirm the structure of the benzoxazine. The detailed assignment of aromatic peaks in Figures 2, assisted by the correlation in ^1H-^1H COSY, and ^1H-^{13}C HETERCOR (Supporting Information Figures S6 and S7), confirms the structure of **F-ap**.

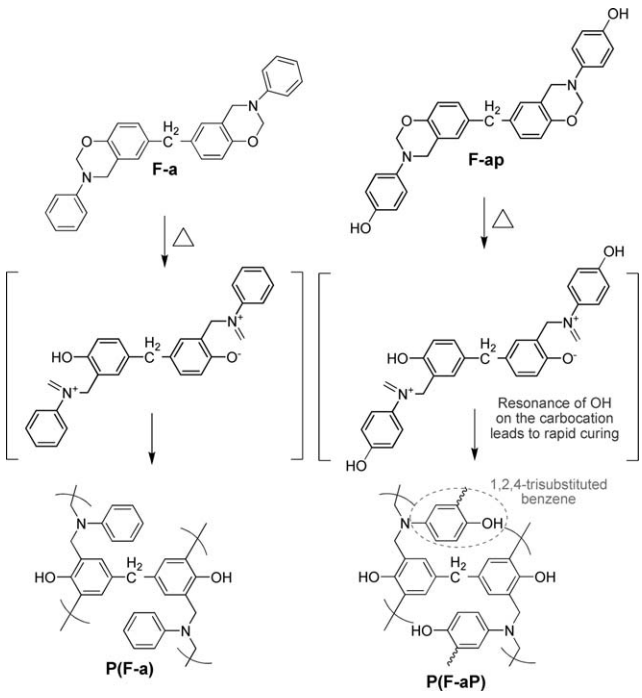

SCHEME 2 Ideal structure of benzoxazine thermosets, P(**F-a**) and P(**F-ap**).

TABLE 1 Thermal Properties of the Resulting Thermosets

Thermoset ID	T_g (DMA)[a]	T_g (DSC)[b]	$T_{d5\%}$[c]	Char Yield[d]
P(**F-a**)	173	162	314	49
P(**F-ap**)	–	220	381	69
F-a/DGEBA	164	155	365	41
F-ap/DGEBA	222	202	392	40
F-a/BMI	204	162	375	50
F-ap/BMI	294	295	410	58

[a] The temperature corresponding to the peak temperature of tan δ, measured by DMA at a heating rate of 5°C/min.
[b] T_g is measured by DSC at a heating rate of 20°C/min.
[c] The temperature corresponding to 5% weight loss in a nitrogen atmosphere, measured by TGA at a heating rate of 20°C/min.
[d] Residual weight % at 800°C in a nitrogen atmosphere.

DSC thermograms of benzoxazines

The DSC thermograms of **F-a** and **F-ap** are shown in Figure 3**. F-ap** shows a melting point of 143°C, and a much lower initial exothermic temperature than that of **F-a**. Endo el al. reported that the stability of the Zwitter ion is crucial to the ring opening of benzoxazine.[27] Ronda et al. also reported that the electron-donating substitute in the para position stabilizes the Zwitter ion, and enhance the reactivity.[28] In this case, the electron-donating phenolic OH in **F-ap** can stabilize the Zwritter ion through resonance. In addition, it has been reported that phenolic OH can catalyze the ring-opening of oxazine.[20,29–31] Both factors shift the exothermic peak to a lower temperature. The rapid curing characteristic can be reflected in the short gel time of **F-ap**. The gel time of **F-ap** at 170°C is less than 1 min, making it difficult to make a void-free sample for DMA measurement.

Curing of F-ap probed by IR

Benzoxazine can be thermally cured into a cross-linked polybenzoxazine through the ring-opening of the benzoxazine linkages. Figure 4 shows the IR spectra of **F-ap** after accumulative curing at each temperature for 20 min. After curing at 180°C, the Ar—O—C absorptions at 1040 and 1240 cm^{-1}, and the oxazine absorption at 1370 cm^{-1} disappeared. The absorptions of the characteristic mode of benzene with an attached oxazine ring at 945 cm^{-1} also disappeared, suggesting a rapid curing characteristic. As the intensity of the aforementioned peaks decreased, the reduction in intensity

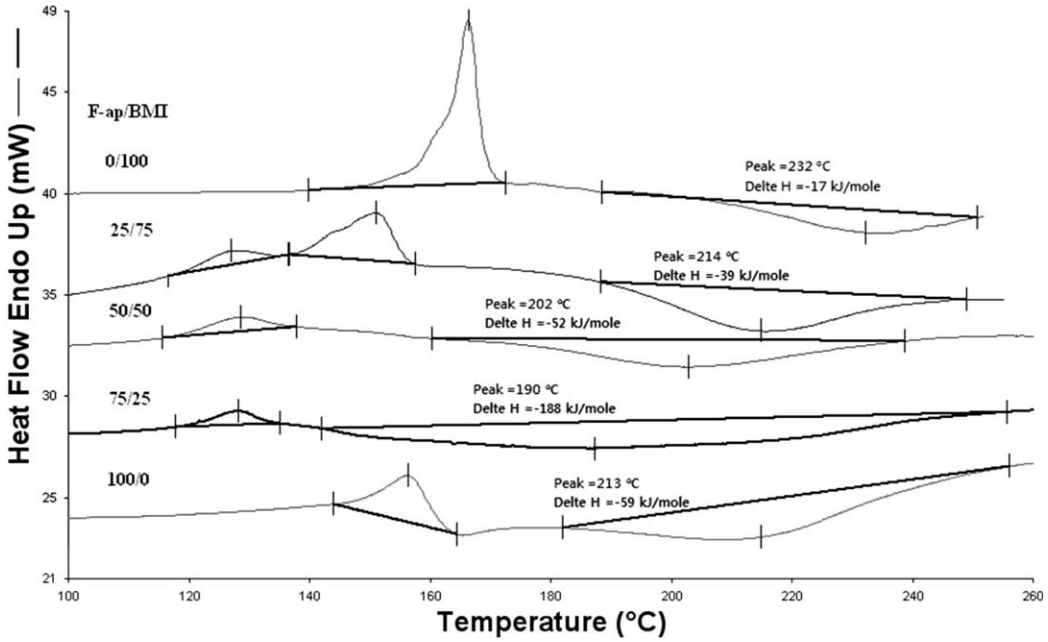

FIGURE 5 DSC heating thermograms of **F-ap**/BMI mixtures.

of 1,2,4-trisubstituted benzene absorption appearing at 1499 cm^{-1} was not obvious. The phenomena can be explained by the compensation of a newly formed 1,2,4-trisubstituted benzene linkage, as marked by a circle in Scheme 2. As shown in Scheme 2, the nitrogen linkage in P(**F-a**) is linked to a phenyl pendant, but the nitrogen linkage in P(**F-a)** is bonded to the other repeating unit, leading to a higher crosslinking density. The higher crosslinking is reflected in the T_g values of P(**F-ap**) and P(**F-a**). DSC shows the T_g of P(**F-ap**) is 220°C (Supporting Information Figure S8), while the T_g of P(**F-a**) is 160°C. However, as mentioned before, the rapid curing characteristic hinders the formation of a void-free sample, so no DMA data for P(**F-ap**) to further support the DSC data. The thermal stability of P(**F-ap**) and P(**F-a**) were evaluated by TGA in a nitrogen atmosphere, and the results are provided in Table 1. The 5 wt% degradation temperature is 314 and 381°C for P(**F-a**) and P(**F-ap**), respectively. The char yield is 49 and 69 wt% for P(**F-a**) and P(**F-ap**), respectively. The higher crosslinking density of P(**F-ap**) than P(**F-a**) is thought to be responsible the for the better thermal stability of P(**F-ap**).

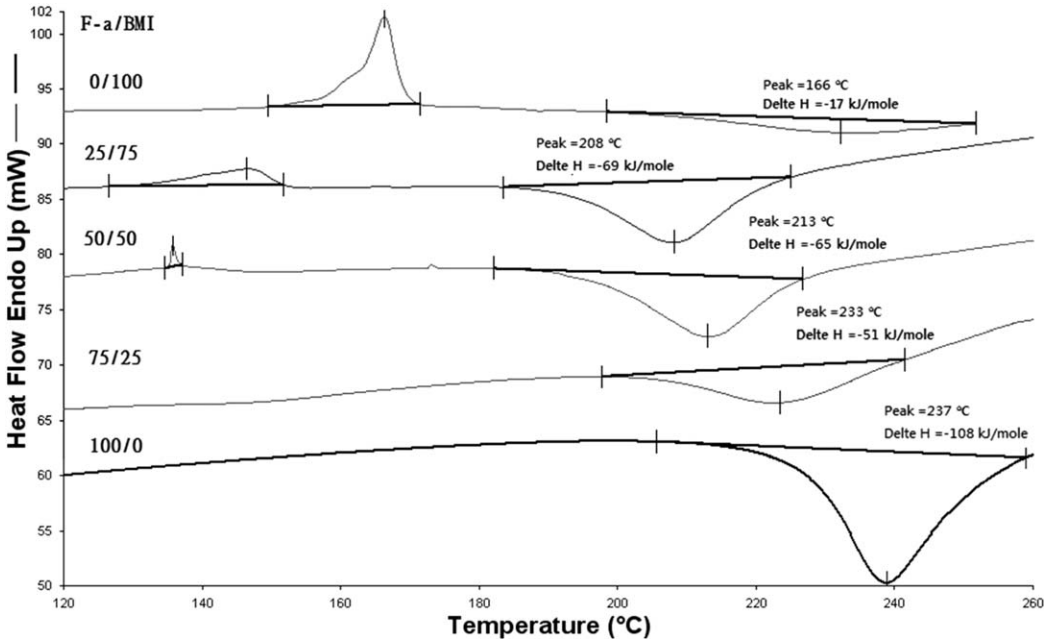

FIGURE 6 DSC heating thermograms of **F-a**/BMI mixtures.

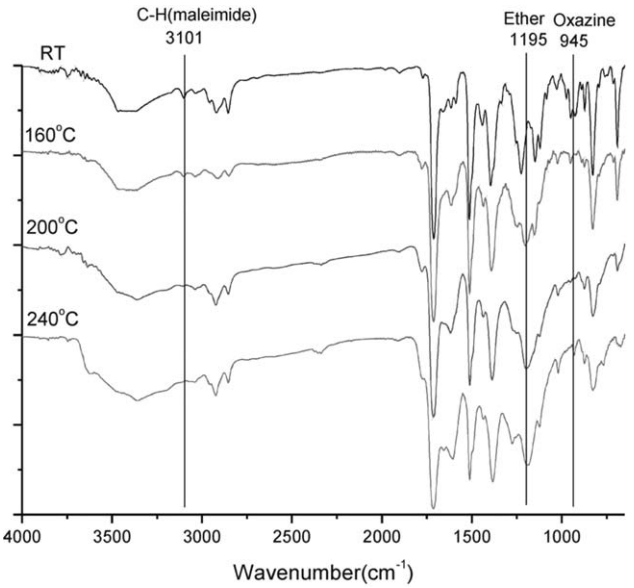

FIGURE 7 IR spectra of the **F-ap**/BMI (50/50) mixture after accumulative curing at each temperature for 20 min.

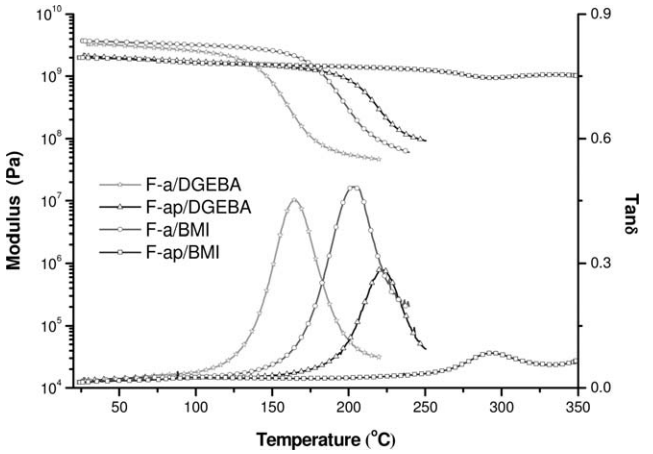

FIGURE 8 DMA thermograms of **F-a-** and **F-ap-**based thermosets.

DSC and IR analyses

Figure 5 shows the DSC heating thermograms of the **F-ap**/BMI powder mixtures. Pristine BMI showed a melting point of 166°C, and an exothermic peak from 200 to 250°C. The exothermic peak temperature of the **F-ap**/BMI powder mixture decreased from 235 to 185°C as the ratio of **F-ap** increased from 0% to 75%. In addition, the exothermic enthalpy was much higher than the enthalpy calculated from linear combination. For example, the measured enthalpy was 59 and 17.3 kJ/mole for **F-ap** and BMI, respectively. The calculated enthalpy was 27 and 38 kJ/mol, respectively, for the 25/75 and 50/50 mixtures. However, the enthalpy measured was 39 and 52 kJ/mol, respectively for the 25/75 and 50/50 mixtures. The larger enthalpy suggests co-reaction occurred in addition to the hompolymerizaiton of **F-ap** and BMI. Figure 6 shows the DSC heating thermograms of the **F-a**/BMI powder mixtures. The forward exothermic temperature was not as obvious as that in the **F-ap**/BMI system. This indicates that the obvious forward exothermic temperature in Figure 5 is related to the co-reaction between phenolic OH and maleimide. The result is consistent with the observation of Takeichi et al.[23]

Figure 7 shows the IR spectra of the **F-ap**/BMI (50/50) mixture after accumulative curing at each temperature for 20 min. The C═**CH** absorption of maleimide at 3101 cm^{-1} and oxazine absorption at 945 cm^{-1} decreased simultaneously,

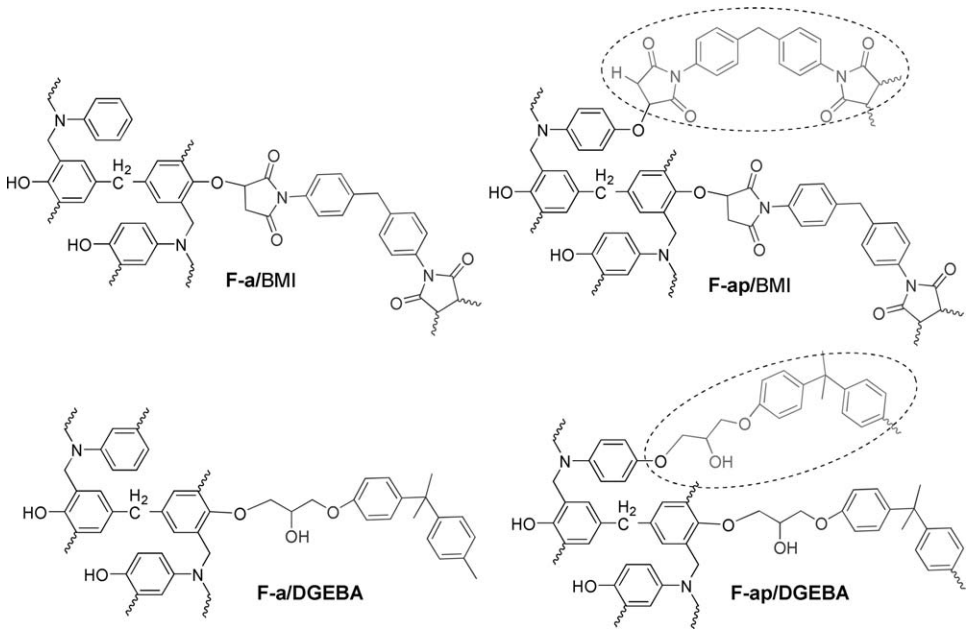

SCHEME 3 Ideal structure of benzoxazine/BMI and benzoxazine/DGEBA thermosets.

and disappeared after curing at 200°C. An ether absorption at 1195 cm^{-1} appeared rapidly with the progress of curing, indicating a ph—O—C bond was formed. Similar results were found in the 75/25 and 25/75 compositions (Supporting Information Figures S9–S10). This result is consistent with that observed by Takeichi et al.[23]

Thermal properties of thermosets

Figure 8 shows the DMA thermograms of the **F-a**/BMI and **F-ap**/BMI thermosets. Only one tan δ peak was observed, indicating that a homogeneous copolymer was obtained. The T_g of **F-ap**/BMI thermoset was as high as 294°C, which is 90°C higher than that of the **F-a**/BMI thermoset. The result demonstrates the high-T_g advantage of the **F-ap**-based thermosets. The high-T_g characteristic of the **F-ap** based thermoset can also be supported by the DMA data of the **F-a**/DGEBA and **F-ap**/DGEBA thermosets (Fig. 8). As shown in the figure, the T_g of the **F-ap**/DGEBA thermoset was 222°C, which is 58°C higher than that of the **F-a**/DGEBA thermoset. Since **F-ap** and **F-a** exhibit a similar structure except for the phenolic OH linkages, the higher T_g of the **F-ap**-based thermoset is thought to be related to the extra crosslinking point provided by the extra phenolic OH, as marked by a circle in Scheme 3. The smaller tan δ height supports the more rigid structure of the **F-ap**/BMI thermoset than that of the **F-a**/BMI thermoset. The same result was also observed in the **F-ap**/DGEBA and **F-a**/DGEBA systems. Compared with the data with those in our previous work,[32] P(**F-ap**) shows lower T_g than P(P-bapf), but the phenolic OHs of **F-ap** make the T_g can be significant enhanced through copolymerization with BMI.

The 5% degradation temperature of the **F-ap/**BMI thermoset was 410°C, which is higher than that of the **F-a/**BMI thermoset (375°C) (Supporting Information Figure S11, Table 1). The larger number of crosslinking sites between **F-ap** and BMI might be responsible for the better thermal stability of the **F-ap/**BMI thermoset. A similar result was observed for the **F-ap**/DGEBA and **F-a**/DGEBA thermosets. The 5% degradation temperature of the **F-ap/**DGEBA thermoset was 392°C, which was higher than that (365°C) of the **F-a/**DGEBA thermoset (Supporting Information Figure S12). According to the literature, the release of aniline fragments is responsible for the low thermal stability of biphenol and aniline-based polybenzoxazines.[33] In contrast, the nitrogen linkage in the **F-ap-**based thermoset is bonded to the other repeating unit, as shown by the circled structure in Scheme 3. This makes the release of aniline fragments difficult, and causes the **F-ap-**based thermoset to be thermally more stable than the **F-a-**based thermoset.

CONCLUSIONS

A bifunctional benzoxazine (**F-ap)** with precisely two phenolic OHs was successfully prepared. Due to the resonance of phenolic OH on the Zwitter ion, **F-ap** exhibited a rapid curing characteristic, as supported by the data of the DSC thermogram, IR spectra, and gel time. The IR spectra of the **F-ap**/BMI mixture showed that ether linkage (ph—O—C) was formed between the co-reaction of the phenolic OH and maleimide. Compared to **F-a**, the phenolic OHs of **F-ap** provided extra reaction sites with epoxy and bismaleimide. Therefore, **F-ap** based thermosets show higher T_g and better thermal stability than **F-a** based thermosets. The combination of the rapid curing characteristic, high T_g, and good thermal stability makes the **F-ap** attractive for electronic applications, especially in the field of copper clad laminates.

ACKNOWLEDGMENT

The authors thank the National Science Council of the Republic of China, Taiwan, for financial support.

REFERENCES AND NOTES

1 N. N. Ghosh, B. Kiskan,Y. Yagci, *Prog. Polym. Sci.* **2007**, *32*, 1344–1391.

2 X. Ning, H. Ishida, *J. Polym. Sci. Part A: Polym. Chem.* **1994**, *32*, 1121–1129.

3 C. F. Wang, Y. C. Su, S. W. Kuo, C. F. Huang, Y. C. Sheen, F. C. Chang, *Angew. Chem. Int. Edit.***2006**, *45*, 2248–2251.

4 A. Chernykh, T. Agag, H. Ishida, *Macromolecules* **2009**, *42*, 5121–5127.

5 K. D. Demir, B. Kiskan, Y. Yagci, *Macromolecules* **2011**, *44*, 1801–1807.

6 Y. L. Liu, C. I. Chou, *J. Polym. Sci. Part A: Polym. Chem.* **2005**, *43*, 5267–5282.

7 T. Agag, T. Takeichi, *Macromolecules* **2003**, *36*, 6010–6017.

8 T. Agag, T. Takeichi, *Macromolecules* **2001**, *34*, 7257–7263.

9 T. Takeichi, S. Thongpradith, S. Hirai, T. Takiguchi, T. Kawauchi, *High Perform. Polym.* **2012**, *24*, 765–774.

10 T. Agag, J. Liu, R. Graf, H. W. Spiess, H. Ishida, *Macromolecules*, **2012**, *45*, 8991–8997.

11 H. Oie, A. Mori, A. Sudo, T. Endo, *J. Polym. Sci. Part A: Polym. Chem.* **2012**, *50*, 4756–4761.

12 Y. L. Liu, J. M. Yu, *J. Polym. Sci. Part A: Polym. Chem.* **2006**, *44*, 1890–1899.

13 R. Andreu, J. A. Reina, J. C. Ronda, *J. Polym. Sci. Part A: Polym. Chem.* **2008**, *46*, 6091–6101.

14 L. Jin, T. Agag, Y. Yagci, H. Ishida, *Macromolecules* **2011**, *44*, 767–772.

15 W. H. Hu, K. W. Huang, S. W. Kuo, *Polym. Chem.* **2012**, *3*, 1546–1554.

16 T. Agag, C. R. Arza, F. H. J. Maurer, H. Ishida, *Macromolecules* **2010**, *43*, 2748–2758.

17 H. Oie, A. Sudo, T. Endo, *J. Polym. Sci. Part A: Polym. Chem.* **2011**, *49*, 3174–3183.

18 H. Takemura, A. Takahashi, H. Suga, M. Fukuda, T. Iwanaga, *Eur. J. Org. Chem.* **2011**, *2011*, 3171–3177.

19 T. Agag, T. Takeichi, *J. Polym. Sci. Part A: Polym. Chem.* **2007**, *45*, 1878–1888.

20 T. Agag, T. Takeichi, *High Perform. Polym.* **2001**, *13*, S327–S342.

21 T. Agag, T. Takeichi, *J. Polym. Sci. Part A: Polym. Chem.* **2006**, *44*, 1424–1435.

22 Y. L. Liu, J. M. Yu, C. I. Chou, *J. Polym. Sci. Part A: Polym. Chem.* **2004**, *42*, 5954–5963.

23 T. Takeichi, Y. Saito, T. Agag, H. Muto, T. Kawauchi, *Polymer* **2008**, *49*, 1173–1179.

24 C. H. Lin, S. L. Chang, C. W. Hsieh, H. H. Lee, *Polymer* **2008**, *49*, 1220–1229.

25 C. H. Lin, S. L. Chang, H. H. Lee, H. C. Chang, K. Y. Hwang, A. P. Tu, W. C. Su, *J. Polym. Sci. Part A: Polym. Chem.* **2008**, *46*, 4970–4983.

26 C. S. Marvel, N. Tarköy, *J. Am. Chem. Soc.* **1957**, *79*, 6000–6002.

27 R. Kudoh, A. Sudo, T. Endo, *Macromolecules* **2010**, *43*, 1185–1187.

28 R. Andreu, J. A. Reina, J. C. Ronda, *J. Polym. Sci. Part A: Polym. Chem.* **2008**, *46*, 3353–3366.

29 M. A. Espinosa, M. Galià,V. Cádiz, *Polymer* **2004**, *45*, 6103–6109.

30 M. A. Espinosa, V. Cádiz, M. Galiá, *J. Polym. Sci. Part A: Polym. Chem.* **2004**, *42*, 279–289.

31 M. A. Espinosa, V. Cádiz, M. Galià, *J. Appl. Polym. Sci.* **2003**, *90*, 470–481.

32 H. C. Chang, C. H. Lin, Y. W. Tian, Y. R. Feng, L. H. Chan, *J. Polym. Sci. Part A: Polym. Chem.* **2012**, *50*, 2201–2210.

33 K. Hemvichian, H. Ishida, *Polymer* **2002**, *43*, 4391–4402.